

The origin of methane in the East Siberian Arctic Shelf unraveled with triple isotope analysis

^{1,2}Célia J. Sapart*, ^{3,4}Natalia Shakhova, ^{3,4,5}Igor Semiletov, ^{1,6}Joachim Jansen, ⁷Sönke Szidat, ⁵Denis Kosmach, ⁵Oleg Dudarev, ¹Carina van der Veen, ⁸Matthias Egger, ⁹Valentine Sergienko, ⁵Anatoly Salyuk, ¹⁰Vladimir Tumskey, ²Jean-Louis Tison and ¹Thomas Röckmann.

¹Institute for Marine and Atmospheric research Utrecht (IMAU), Utrecht University, Princetonplein 5, 3584CC Utrecht, The Netherlands.

²Laboratoire de glaciologie, Université Libre de Bruxelles (ULB), Avenue Roosevelt 50, 1050 Brussels, Belgium.

³University Alaska Fairbanks, International Arctic Research Center, 930 Koyukuk Drive, Fairbanks, USA, 99775.

⁴Tomsk Polytechnic University, 30 Prospect Lenina, Tomsk, Russia.

⁵Russian Academy of Sciences, Far Eastern Branch, V.I. Il'ichov Pacific Oceanological Institute, 43 Baltiyskaya street, Vladivostok 690041.

⁶Department of Geological Sciences and Bolin Centre for Climate Research, Stockholm University, Svante Arrhenius väg 8, SE 114 18, Stockholm, Sweden.

⁷Department of Chemistry and Biochemistry & Oeschger Centre for Climate Change Research, University of Bern, Freiestrasse 3, CH-3012 Bern, Switzerland.

⁸Center for Geomicrobiology, Department of Bioscience, Aarhus University, Ny Munkegade 114, 8000 Aarhus, Denmark

⁹Russian Academy of Sciences, Far Eastern Branch, Institute of Chemistry, 159 Prospect 100-letiya Vladivostoka, Vladivostok 690022.

¹⁰Moscow State University, 1 Leninskie Gori, 119991, Moscow, Russia.

Abstract

The Arctic Ocean, especially the East Siberian Arctic Shelf (ESAS) has been proposed as a significant source of methane that might play an increasingly important role in the future. However, the underlying processes of formation, removal and transport associated with such emissions are to date strongly debated.

CH₄ concentration and triple isotope composition were analyzed on gas extracted from sediment and water sampled at numerous locations on the shallow ESAS from 2007 to 2013. We find high concentrations (up to 500 μM) of CH₄ in the pore water of the partially thawed subsea permafrost of this region. For all sediment cores, both hydrogen and carbon isotope data reveal the predominant occurrence of CH₄ that is not of thermogenic/natural gas origin as it has long been thought, but resultant from microbial CH₄ formation. At some locations meltwater from buried meteoric ice and/or old organic matter preserved in the subsea permafrost were used as substrates.

44 Radiocarbon data demonstrate that the CH₄ present in the ESAS sediment is
45 of Pleistocene age or older, but a small contribution of highly ¹⁴C-enriched
46 CH₄, from unknown origin, prohibits precise age determination for one
47 sediment core and in the water column. Our sediment data suggest that at
48 locations where bubble plumes have been observed, CH₄ can escape
49 anaerobic oxidation in the surface sediment.

50

51 **1.Introduction**

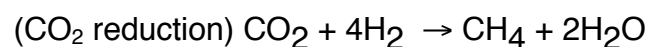
52

53 The Arctic subsea permafrost harbors a very large active carbon pool
54 of similar size as the terrestrial Siberian permafrost reservoir (Shakhova et al.,
55 2010a). Between 12 and 5kyr Before Present (BP), the Holocene
56 transgression (Bauch et al, 2001) submerged extensive parts of the
57 Pleistocene age terrestrial permafrost in Northern Siberia, forming the very
58 shallow ESAS (Romanovskii et al., 2005). As a result, the formerly terrestrial
59 permafrost has been continuously exposed to increasing seawater
60 temperature, salt and anoxic conditions (Dimitrenko et al., 2011, Nicolsky et
61 al., 2012) allowing the remobilization of carbon from the Pleistocene
62 reservoirs. The four suggested mechanisms controlling the release of
63 Pleistocene carbon to the ESAS are the deepening of the permafrost level,
64 gas hydrate degradation, coastal erosion and riverine discharge (e.g.
65 Shakhova et al., 2005, 2009, 2010a,b, 2015; O'Connor et al., 2010,
66 Winterfeld et al., 2015, James et al., 2016). Holocene age carbon originating
67 mainly from coastal erosion and riverine discharge (Charkin et al., 2011;
68 Semiletov et al., 2012; Karlsson et al., 2011, 2016) has accumulated on the
69 ESAS shelf and overlays the Pleistocene age sediment (Vonk et al., 2012,
70 2014 ; Feng et al., 2013).

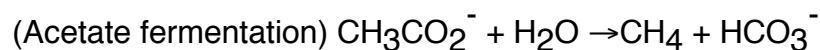
71 Under anaerobic conditions and depending on its type and quality
72 (Schuur et al., 2013), the remobilized carbon can be used to produce CH₄.
73 Microbial CH₄ is produced by methanogenesis using as main substrates
74 carbon dioxide (CO₂) or acetate according to the following reactions (Whiticar,
75 1999):

76

77



78



79 In the deep Earth layers, CH₄ can also be formed through thermal
80 degradation of organic matter (e.g. Schoell, 1988) and migrate towards the
81 surface. This CH₄ is considered thermogenic. A large part of the CH₄ formed
82 in the seafloor is removed by anaerobic oxidation with seawater sulfate in
83 sediments (e.g. Reeburgh, 2007, Knittel and Boetius, 2009) or in the water
84 column where CH₄ can be consumed by aerobic methanotrophic bacteria
85 under specific nutrient and redox conditions (e.g. Kessler et al., 2011, Mau et
86 al., 2013, Steinle et al., 2015). Each type of CH₄ formation/removal pathway
87 produces CH₄ with a characteristic isotopic signature ($\delta^{13}\text{C}$ and δD)
88 depending on the isotopic composition of the substrate and the kinetic isotope

89 effect associated with the respective chemical reaction involved.
90 Microorganisms need less energy to metabolize molecules with smaller bond
91 energy, which leads to discrimination against heavy isotopes. Therefore, CH₄
92 produced by methanogenesis has a lighter isotopic signature than its
93 substrates but when it is consumed, its remaining reservoir will become more
94 enriched in heavy isotopes (e.g. Whiticar 1999, Conrad, 2005). Diffusive
95 transport can also cause isotopic discrimination, because lighter
96 isotopologues diffuse faster than heavier ones. However, this fractionation is
97 relatively small (<5‰: Fuex, 1980, <20‰: Prinzhofer and Pernaton, 1997 and
98 3‰: Chanton et al. 2005) compared to the isotopic fractionation associated
99 with methanogenesis (7-95‰ for δ¹³C and 260-430‰ for δD) and with CH₄
100 oxidation (2-39‰ for δ¹³C and 66-350‰ for δD) (Whiticar, 1999, Holler et al.,
101 2009).

102 Shakhova et al., 2010b, have shown that CH₄ concentrations in the
103 ESAS water were anomalously high (up to 500 nM) compared to CH₄ values
104 generally observed in ocean waters (~5 nM, Damm et al., 2008). Vigorous
105 bubbling events (1.5 to 5.7 bubbles per second) were observed at some sites
106 (Shakhova et al., 2013) as well as seepages of thermogenic CH₄ (Cramer
107 and Franke, 2005) indicating that part of the water column supersaturation
108 likely results from a seabed source. The destabilization of gas hydrates is
109 frequently discussed as CH₄ source in this region (e.g. Kvenvolden, 1988,
110 Romanovskii et al., 2005, Shakhova et al., 2010a, Ruppel and Kessler, 2016),
111 however, important gaps exist in the assessment of the quantity and the
112 nature of the CH₄ stored or formed in the Arctic seabed (e.g. Ruppel et al.,
113 2014).

114 To disentangle the origin(s) of this CH₄ anomaly, we measured CH₄
115 concentration, stable isotope composition and (on selected samples)
116 radiocarbon content in sediment and water samples from several winter
117 campaigns and summer cruises from 2007 to 2013 on the ESAS shelf and
118 shelf edge. While stable isotope analyses help identify the chemical
119 pathways involved in CH₄ removal and formation processes, radiocarbon
120 measurements give information on the age of the CH₄ substrate. The
121 combination of the isotope information thus helps in determining the possible
122 origin(s) of this gas. Determining the stable isotope signatures of the main
123 methane sources in the ESAS remains as well crucial to better quantify the
124 CH₄ emissions in this region using isotopic- and back-trajectory analysis of
125 atmospheric CH₄ (Thornton et al., 2016).

126

127

128 **2.Method**

129

130 **2.1.Drilling and sediment sampling**

131

132 Summer surface sediment drilling and water sampling campaigns were
133 carried out on research vessels while the winter field campaigns were
134 accomplished using an equipment caravan, which traveled over the sea ice to
135 the drilling locations. In the latter case, casings were drilled through the fast
136 ice into the seabed, allowing dry drilling using a rotary drill with 4 m casing

137 with a newly built URB-4T drilling rig (made in 2011 by the Vorovskii Factory
138 for Drilling Equipment, Ekaterinburg, Russia). Thawed and frozen sediments
139 for each core were subsampled straight after (i.e. maximum a few minutes
140 after) the drilling using ice screws for frozen samples and a heavy plastic
141 syringe-like sampler for thawed samples at 20 cm vertical resolution.

142 **2.2. Gas extraction and measurement in sediments**

143 Sediment subsamples were subsequently immersed in glass vials filled
144 with a saturated sodium chloride solution to drive gases out of solution and
145 capped with a septum for equilibration in an ultrasonic water bath at a
146 temperature of 20°C. The gas chromatograph (GC) used to measure CH₄
147 concentrations was equipped with two 10-Port gas sampling valves, a 2 m
148 MolSieve 13X column, a 30 m capillary column and a 6 channel PeakSimple
149 data system. A flame ionization detector (FID) was used for concentrations of
150 CH₄ <200 ppm and a thermal conductivity detector (TCD) for concentrations
151 of CH₄ >200 ppm. The GC oven was operated isothermally at 40°C and the
152 maximum detector temperature was held at ≈ 250°C. The carrier gas used
153 was helium. Daily calibration was performed with certified 1.96 ppm and
154 99.999 ppm CH₄ gas standards from Air Liquide, USA. The standard
155 deviation of duplicate analyses (three to five replicates) was <2%.
156 Reproducibility was ~1% based on multiple standard injections during daily
157 calibrations. The concentration of dissolved CH₄ in the water and sediment
158 samples was calculated with the Bunsen solubility coefficient for CH₄
159 (Wiesenburg and Guinasso, 1979) for the appropriate equilibration
160 temperature, pressure and the volume of headspace and water/sediment in
161 each vial.

162 The stable isotope measurements were performed using a Continuous
163 Flow Isotope Ratio Mass Spectrometry (CF-IRMS) system as described in
164 Brass and Röckmann, 2010 and Sapart et al., 2011. Radiocarbon analyses
165 could be performed only on the largest samples (containing more than 20 µg
166 of CH₄). In that case, CH₄ was preconcentrated and combusted to CO₂. The
167 ¹⁴C content of the CO₂ was measured by accelerator mass spectrometry
168 (Szidat et al., 2014) using a specific gas inlet (Ruff et al., 2010).

169

170 **2.3. Gas extraction and measurement from seawater samples**

171

172 Water samples were collected directly from the Niskin bottles. Gas
173 from seawater samples was extracted using a modified headspace vacuum-
174 ultrasonic degassing method (Schmitt et al., 1991, Lammers et al., 1994). The
175 gas released was accumulated in an evacuated burette to measure its
176 quantity and was then transferred into a smaller flask for storage, and
177 analysed as described in Section 2.2.

178

179 **3. Results and discussion**

180

181 We present results of CH₄ concentrations, stable isotope composition
182 and (on selected samples) radiocarbon content on four shallow sediment
183 cores (<3m), four deep sediment cores (ID-11, IID-13, IIID-13, VD-13) (down
184 to a maximum depth of 53m in the Buor-Khaya Bay (BKB)) and about fifty
185 water samples from four coastal areas of the ESAS: the Lena Delta (LD),
186 BKB, the Dmitry Laptev Strait (DLS) and the Shelf Edge (SE) (Fig.1) (see
187 Table S1 for more detail on the sample locations). Because of the harsh field
188 and weather conditions during this campaign, no sediment drilling was
189 possible at the SE, hence only water data are presented for this site. All
190 water and sediment sampling, except for the ID-11 core, was performed at
191 hotspot sites, i.e., at locations where active gas bubbling from the seafloor
192 and high concentrations of dissolved CH₄ were previously observed as
193 discussed in Shakhova et al., 2010a. The location of core ID-11 is therefore
194 referred to as 'non-ebullition site'. This core as well as the IIID-core were
195 thawed all the way down (>50 m) while the IID-13, and VD-13 cores were
196 thawed down to 19 and 12m, respectively. Note that for the two latter cores,
197 sampling was continued through the deeper frozen sediment to 30 and 35m
198 respectively. For more details on the lithology, the cryostructure and the
199 sediment properties, see SI, section 1 and Fig.S1-S4.

200

201 **3.1 CH₄ formation pathways in the sediment**

202

203 Depth profiles of CH₄ concentration, stable isotope composition ($\delta^{13}\text{C}$
204 and δD) and the radiocarbon content (in percent modern carbon, pmC) are
205 presented in Fig.2. In both hotspot and non-ebullition cores, CH₄
206 concentrations are far above values observed in the water column and CH₄
207 is strongly depleted in heavy stable isotopes in all sediment cores. CH₄ in the
208 hotspot cores IID-13, IIID-13 and VD-13 is more depleted in D and slightly
209 more enriched in ¹³C than in the non-ebullition core. These differences can be
210 caused by the distance of the drill sites from the coast, the amount of time
211 each site has been inundated and the differences in lithology (SI, section 1).
212 These factors will play a role on the substrate availability (Karlsson et al.,
213 2011, 2016, Tesi et al., 2014, 2016). We will focus the discussion on the
214 origin of the substrate(s) for each core below.

215

216 The expected stable isotope signatures of the three potential CH₄
217 formation pathways in marine sediment (e.g. Whiticar, 1999): CO₂ reduction,
218 acetate fermentation and thermal degradation of organic matter are depicted
219 together with our water and sediment stable isotope data in a dual isotope
220 plot (Fig.3). Overall, the deep sediment core data (diamonds) fall in between
221 the isotope source signatures of the two main microbial CH₄ formation
222 pathways: carbonate reduction and acetate fermentation. These atypical
223 stable isotope signatures could imply that CH₄ is formed by a mixture of both
224 microbial pathways or/and by using different substrates from the ones
225 considered in Whiticar, 1999. It is unlikely to be explained by physical
226 alteration (e.g. diffusion, gravitational settling) because these processes
227 would result in equal fractionation for the CH₃D and ¹³CH₄ isotopologues.

227

228 For the non-ebullition core ID-11, most of the $\delta^{13}\text{C}$ values are typical
(though on the light end side) of the reduction of carbonates, but about 2/3 of

229 the samples show δD values that are considered too low (down to about -
230 60‰) for such a pathway. The most enriched δD data correspond to the top
231 of this core and are discussed in section 3.2. For this core, salinity
232 measurements (from 20 PSU at the surface to 13 PSU at depth) indicate the
233 presence of interstitial seawater all the way down the core. When the
234 seawater sulfate enters the marine sediment, it provides sulfate reducing
235 bacteria with the electron acceptor they need to outcompete methanogens for
236 acetate (Lessner, 2009). This indicates that for this core *in situ* (i.e. at the
237 depth where the samples were taken) acetoclastic CH_4 formation may be
238 suppressed, despite an abundance of organic material. CO_2 and water
239 remains therefore the most likely non-competitive substrate for methanogens
240 if CH_4 formation would occur in the thawed permafrost. In that case, the very
241 light δD values can be due to 1) a mixture of carbonate reduced (formed *in*
242 *situ* or not) and acetoclastic (migrating vertically or horizontally) CH_4 or 2) the
243 use of isotopically depleted hydrogen substrate for CH_4 formation by
244 carbonate reduction. On the dual isotope plot (Fig.2), the area of the
245 carbonate reduction pathway considers modern seawater as water substrate
246 for carbonate reduction. However the meltwater present in subsea permafrost
247 originates from buried meteoric ice with much more depleted $\delta D(H_2O)$
248 signatures. Chanton et al. (2006) and Brosius et al. (2012) reported values
249 for $\delta D(H_2O)$ of $-135 \pm 25\text{‰}$ and $-220 \pm 30\text{‰}$, respectively in old Arctic permafrost.
250 This is about 200‰ to 105‰ more depleted in deuterium than modern Arctic
251 seawater (Friedman et al., 1964). We suggest that methanogens present in
252 the thawing permafrost (Koch et al., 2009) use and/or have used such
253 depleted permafrost meltwater or unfrozen porewater as a hydrogen source
254 to form CH_4 with low δD values as it is observed in the non-ebullition core.

255 For the hotspot cores IID-13 IIID-13 and VD-13, the δD values are
256 characteristic of acetate fermentation, but the $\delta^{13}C$ signatures are about 30‰
257 more depleted in ^{13}C in comparison to what has been measured previously
258 from this pathway (e.g. Whiticar, 1999, Walter et al., 2008). This depletion in
259 ^{13}C must originate from 1) the addition of carbonate reduced CH_4 to an
260 acetoclastic pool or/and 2) the recycling of CH_4 after AOM-mediated carbon
261 isotope equilibrium under sulfate limitation conditions (Yoshinaga et al., 2014,
262 Geprägs et al., 2016). For the latter, the ^{13}C depletion must be accompanied
263 by a decrease in CH_4 concentration, but this was not observed: the CH_4
264 concentrations in our cores were relatively constant and not correlated with
265 the $\delta^{13}C$ values (Fig.4). For these cores, because of the harsh conditions in
266 the field, no reliable sulfate and salinity profiles could be retrieved, so
267 unfortunately no sulfate data are available to support the interpretation.

268 The ^{14}C content of CH_4 from the hotspot cores covers a range from
269 0.79 to 3.4pmC corresponding to a radiocarbon age of 26 to 39kyBP (Fig.2).
270 This indicates a carbon substrate of Pleistocene age. For the ID-11 non-
271 ebullition core, ^{14}C values are unexpectedly high and vary from 87pmC
272 (radiocarbon age=1kyBP) to 2367pmC (Fig.2), which represents a substantial
273 enrichment above the natural background. The same applies to water
274 samples from the SE. Note that levels close to 100pmC indicate modern
275 values. Even samples that had been affected by the nuclear bomb testing in
276 the 1950s and 1960s would show levels below 200pmC, thus ^{14}C values

277 >200pmC cannot be caused by known natural processes. As discussed in the
278 SI section 2, local anthropogenic nuclear contribution, e.g. from nuclear waste
279 buried in the coastal permafrost, is the most likely explanation for these
280 elevated radiocarbon levels. The drilling location is shallow (12.5 m) and very
281 difficult to reach hence waste burial is very unlikely to have occurred directly
282 in this area. Moreover the highest contamination is observed at 30 m depth in
283 the sediment showing that it may not originate from the surface. Our first
284 suggestion is that this anthropogenic contamination has been laterally
285 transported in the pore-water of the thawing subsea permafrost in the form of
286 CH₄ or of one of its precursors (e.g. dissolved inorganic carbon) from the
287 coastal terrestrial permafrost to our drilling site (see SI section 2 for more
288 detailed). More data, e.g. of other radionuclides would be essential to confirm
289 this assumption.

290 The shallow sediment samples from hotspot sites have ¹⁴CH₄ values
291 from 3 to 88pmC (radiocarbon age = 1-26kyBP) showing the presence of old
292 CH₄ in surface sediment of relatively modern age and thus confirming the
293 migration of old gas from deeper layers towards the surface. Note that the
294 overall low content of organic carbon (<2.3%) with a high fraction of lignin
295 (Bröder et al., 2016; Vonk et al., 2014) in the surface sediment (Fig.5) and the
296 likely presence of sulfate, would severely inhibit CH₄ formation in the marine
297 layer hence *in situ* methanogenesis there is highly unlikely.

298 We conclude that the CH₄ present in the surface thawed subsea-
299 permafrost is formed mainly microbially. For the non-ebullition core, our
300 observations imply that CH₄ is at least partly not formed *in situ* in thawed
301 subsea permafrost but that it migrates vertically or laterally to the surface of
302 the partially thawed ESAS subsea permafrost. For the hotspot cores, which
303 are closer to the shore and more recently inundated (Table S.1), most of the
304 methane present is of acetoclastic origin and formed with Pleistocene carbon
305 remobilized in the thawing subsea permafrost.

306
307

308 **3.2. CH₄ removal pathways in the sediment**

309

310 The ID-11 non-ebullition site was the only coring location where no
311 active bubbling was observed from the surface sediment. Here, the top 5.8m
312 consist of a thick silty-clay layer (Fig.S1) of marine origin as indicated by the
313 higher salinity and silica concentrations (Fig.5), typical of a marine
314 environment enriched in diatoms. The increase in sulfate concentration
315 together with the strong CH₄ concentration decrease and the isotopic
316 enrichment in both ¹³C and D towards the sediment surface indicate that most
317 of the CH₄ diffusing through this thick Holocene marine layer is removed by
318 anaerobic oxidation with sulfate in the surface sediment before reaching the
319 water column.

320 This marine layer may also act as a physical barrier preventing gas to
321 migrate towards the surface directly. The increase in CH₄ concentration from
322 9 to 5.8m depth without strong isotopic shifts (Fig. 5) and the acoustic data
323 (Fig. 6) show that gas accumulates under this less permeable layer. Part of
324 this gas might migrate laterally and be released to the water at locations

325 where the marine clay layer is thinner or absent. The isotopic signatures of
326 the CH₄ in the pore water of the hotspot cores do not show isotopic
327 fractionation toward the surface (Fig.2). At these sites, ebullition processes
328 may disturb the sulfate-reducing layer and advection may occur. This would
329 reduce the amount of CH₄ subject to anaerobic oxidation (only dissolved CH₄
330 is accessible for methanotrophic organisms) and allow direct gas release to
331 the water column.

332 Overduin et al., 2015 have reported CH₄ concentration and δ¹³C values
333 measured on one sediment core drilled in the Buor-Khaya Bay. The carbon
334 isotopic signature of that core was typical of acetate fermentation in the
335 frozen part of the core, but they observed a strong enrichment in ¹³C
336 associated with a decrease in CH₄ concentration directly above the ice-
337 bonded permafrost. They concluded that CH₄ was strongly oxidized in the
338 thawed subsea permafrost before reaching the water column. Our dataset
339 suggests that the Overduin et al. core is not typical for the entire region as we
340 did not observe similar enrichment in either D or ¹³C associated with a
341 decrease in CH₄ concentration at the ice-bonded permafrost table for the
342 partly frozen cores IID-13 and VD-13 (Fig. 2 and Fig. S.2 and S.4).

343

344 **3.3. CH₄ in the water**

345

346 Compared to the sediment samples, CH₄ in the water samples is more
347 enriched in heavy isotopes. The highest CH₄ concentrations in the water
348 column are observed close to the seabed and at the surface in the presence
349 of sea ice (Fig.2a blue triangles). The ¹⁴C values of water samples are
350 between 83 and 9560pmC (radiocarbon age= 2kyBP to strongly enriched
351 above natural present day values) (Fig.2d) (SI section 2). For the water
352 samples we only encountered the highly enriched ¹⁴CH₄ values at the shelf
353 edge. As demonstrated by the ¹⁴CH₄ data in the non-ebullition core ID-11, this
354 anomaly likely originates from anthropogenic contamination in the sediment.
355 Hence, we suggest that this signature may be diluted over the shelf but
356 becomes indiscernible at locations where strong release of old CH₄ from the
357 sediment occurs. This could explain the broad range of pmC values observed
358 in the water column.

359 Several scenarios may explain the difference in stable isotope
360 signatures between the water- and sediment samples. The first assumes a
361 mixture of microbial CH₄ with a source that is more enriched in heavy
362 isotopes. This source could be either a water source or thermal degradation
363 of organic matter in the Earth's deep crust. In the marine environment, CH₄
364 could in principle be produced at the pycnocline, where natural differences of
365 water density create a "fluid bottom", on which organic particles and pellets
366 could accumulate as substrate for *in situ* methanogenesis (Damm et al., 2008,
367 Karl et al., 2008, Sasakawa et al., 2008). In the ESAS, the pycnocline is very
368 shallow and at the location of sampling, low primary production is expected
369 because of darkness and ice cover in the winter and because of the little
370 available sunlight in the summer due to the high solar zenith angles and the
371 very turbid waters (Semiletov et al., 2016). Bussmann et al. (2013) have
372 investigated the distribution of CH₄ in the estuary of the Lena, one of the

373 largest Russian rivers draining into the ESAS. They reported high CH₄
374 concentrations (up to 1500 nM) in the river and in the creeks draining from
375 permafrost soil and a strong decrease in the Buor-Khaya Bay (down to 26-
376 33nM). They concluded that the CH₄ contained in the rich waters of the river
377 was, for the most part, not reaching the marine waters, but that it was
378 released by diffusion into the atmosphere before reaching the bay. A large
379 water source is therefore unlikely to explain the CH₄ saturation we observe in
380 the ESAS coastal waters.

381 Thermogenic emissions from the sediment are possible, especially
382 from the fault zone near the shelf edge where we find strong heavy isotope
383 enrichment in the water. While we have not measured any CH₄ with a
384 thermogenic stable isotopic signature in our deep sediment cores from the
385 continental shelf, it could be present in the sediments of the shelf edge (which
386 we were unable to sample due to rough field conditions). Moreover, no
387 measurements could be performed directly on gas bubbles (because of the
388 low probability to trap bubbles in the Niskin bottles during sampling), which at
389 the shelf edge might partly originate from thermal degradation of organic
390 matter.

391 The difference between the water and sediment samples may also
392 result from substantial oxidation of the CH₄ emitted from the deep sediment.
393 Such a process should involve enrichments in D and ¹³C associated with a
394 decrease in CH₄ concentration. This pattern is only observed for the winter
395 water samples of the Lena Delta (Fig.4, blue open triangles) where CH₄
396 trapped under the sea ice could be removed by aerobic oxidation. All other
397 water data were collected in the summer and do not show any clear isotopic
398 enrichment correlated with concentration decrease. This could be explained
399 by the continuous addition of CH₄ from the sediment and its direct diffusion
400 from the water into the atmosphere in the summer, especially during storms
401 (Shakhova et al., 2013). These processes as well as water column mixing
402 could mask any oxidative isotope signature.

403 In the winter, CH₄ likely accumulates under the sea ice where the
404 bubble and dissolved phases could equilibrate and aerobic oxidation could
405 occur, while in the summer the gas bubbles will directly reach the atmosphere.
406 In the sediment, gas bubbles have time to equilibrate with pore water,
407 especially when the gas is trapped under relatively impermeable sediment,
408 e.g. the Holocene marine silty-clay layer. Therefore, we assume that in the
409 sediment, the pore water can be in equilibrium with the gas bubbles, while we
410 suggest that in the summer the seawater bubbles may travel too rapidly to
411 reach an isotopic equilibrium with the dissolved gas and to be oxidized. This
412 means that the CH₄ isotopic signature of the gas bubbles may not strongly
413 affect the CH₄ dissolved in seawater, which could also explain the difference
414 observed between the water and sediment stable isotopes values.

415

416 **4. Conclusion**

417

418 Our triple isotope dataset of CH₄ from the sediment and water of the shallow
419 ESAS reveals the presence of CH₄ of microbial origin formed on old carbon
420 with unexpectedly low stable carbon ($\delta^{13}\text{C}$ as low as -108‰) and hydrogen

421 (δD as low as -350‰) isotope signatures down to about 50m under the
422 seabed in the thawed permafrost. These data demonstrate that at locations
423 where a thick marine clay layer is present, this CH_4 is partially oxidized before
424 reaching the seawater. However at locations where ebullition was observed
425 from the seabed, no oxidation was identified in the stable isotope surface
426 sediment profile. In that case and considering the very shallow water column
427 ($<10\text{m}$) in this area, this microbial gas will likely reach the atmosphere when
428 sea ice is absent. Our results show that thawing subsea permafrost of the
429 ESAS emits CH_4 with an isotopic signature that cannot be easily
430 distinguished from Arctic wetland emissions when looking only at stable
431 isotope data. This similarity might complicate recent efforts to quantify Arctic
432 CH_4 source strengths on the basis of isotopic- and back-trajectory analysis of
433 atmospheric CH_4 . Further *in situ* work is necessary – specifically on the
434 isotopic composition of CH_4 in gas bubbles that reach the atmosphere – to
435 better quantify the contribution of the ESAS to the global methane budget.

436

437

438

439

440 **ACKNOWLEDGEMENTS**

441

442 We are grateful to the help of Gary Salazar (University of Bern) with the ^{14}C
443 measurements. This research was supported by the Russian Government
444 (No. 14.Z50.31.0012/03.19.2014), the US National Science Foundation (OPP
445 ARC-1023281; 0909546); the NOAA Climate Program office
446 (NA08OAR4600758). N.S., D.K., and O.D. acknowledge support from the
447 Russian Science Foundation (No. 15-17-20032).

448 We would like to thank Jorien Vonk, Alain Prinzhofer, Helge Niemann, Nadine
449 Mattielli and Dominique Weiss for the fruitful discussions and precious help in
450 the interpretation of these data and Rebecca Fisher, Elise van Winden and
451 Joralf Quist for their help with the stable isotope measurements and system
452 calibration.

453

454

455 **AUTHOR CONTRIBUTION**

456

457 **C.J.S., N.S., T.R., J.J., S.S., I.S., J.L.T. and M.E. worked on the scientific**
458 **interpretation and wrote the manuscript. N.S. and I.S. planned the**
459 **research and organized the multiyear fieldwork campaigns. C.vd.V.,**
460 **C.J.S., S.S. and J.J. performed the isotopic analyses. I.S., D.K., O.D.,**
461 **V.S., A.S. and V.T. performed the water sampling, sediment drilling, the**
462 **headspace preparation and CH_4 concentration measurements on the**
463 **field.**

464

465

466 **REFERENCES**

467

468

469 Bauch, H. A., Mueller-Lupp, T., Taldenkova, E., Spielhagen, R. F., Kassens,
470 H., Grootes, P. M., Thiede, J., Heinemeier, J., & Petryashov, V. V.:
471 Chronology of the Holocene transgression at the North Siberian margin.
472 *Global Planet. Change*, 31, 125-139, 2001.
473
474 Brass, M., & Röckmann, T.: Continuous-flow isotope ratio mass spectrometry
475 method for carbon and hydrogen isotope measurements on atmospheric CH₄,
476 *Atm. Meas. Tech.*, 3, 1707–1721, 2010.
477
478 Bröder, L., Tesi, T., Andersson A., Eglinton T.I., Semiletov I. P., Dudarev O.
479 V., Roos P., Gustafsson Ö. (2016), Historical records of organic matter supply
480 and degradation status in the East Siberian Sea, *Organic Geochemistry*, Vol.
481 91, P. 16-30, 2016.
482
483 Brosius, L. S., Walter Anthony, K. M., Grosse, G., Chanton, J. P.,
484 Farquharson, L. M., Overduin, P. P. & Meyer, H.: Using the deuterium isotope
485 composition of permafrost meltwater to constrain thermokarst lake
486 contributions to atmospheric CH₄ during the last deglaciation. *J. Geophys.*
487 *Res.*, 117, G01022, 2012.
488
489 Bussmann, I.: Distribution of methane in the Lena Delta and Buor-Khaya Bay,
490 Russia, *Biogeosciences*, 10, 4641-4652, 2013.
491
492 Chanton, J. P.: The effect of gas transport on the isotope signature of
493 methane in wetlands, *Organic Geochemistry*, 36, 753–768. 2005.
494
495 Chanton, J. P., Fields, D., & Hines, M. E.: Controls on the hydrogen isotopic
496 composition of biogenic methane from high-latitude terrestrial wetlands. *J.*
497 *Geophys. Res.*, 111, G04004, 2006.
498
499 Charkin A.N.,Dudarev O.V., Semiletov I.P., Kruhmalev A.V., Vonk J.E.,
500 Sánchez-García L., Karlsson E., and Ö. Gustafsson: Seasonal and
501 interannual variability of sedimentation and organic matter distribution in the
502 Buor Khaya Gulf – the primary recipient of input from Lena River and coastal
503 erosion in the SE Laptev Sea, *Biogeosciences*, 8, 2581–941, 2011.
504
505 Cramer, B., and Franke, D.: Indications for an active petroleum system in the
506 Laptev Sea, NE Siberia. *J. Petr. Geology*, 28(4), 369-384, 2005.
507
508 Damm, E., Kiene, R.P., Schwarz, J.,Falck., E & Dieckmann, G.: Methane
509 cycling in Arctic shelf water and its relationship with phytoplankton biomass
510 and DMSP, *Marine Chemistry*, 19, 45-59, 2008.
511
512 Feng, X., Vonk, J. E., van Dongen, B. E., Gustafsson, Ö., Semiletov, I. P.,
513 Dudarev, O. V., Wang, Z., Montluçon, D. B., Wacker, L., & Eglinton, T. I.:
514 Differential mobilization of terrestrial carbon pools in Eurasian Arctic river
515 basins. *PNAS*, 110, 14168-14173, 2013.
516

517 Fuex, A.N.: Experimental evidence against an appreciable isotopic
518 fractionation of methane during migration. In: Douglas, A.G., Maxwell, J.R.
519 (Eds.), *Advances in Organic Geochemistry*, Pergamon, Oxford, 1980.

520
521

522 Friedman, I., Redfield, A. C., Schoen, B., & Harris, J.: The Variation of the
523 Deuterium Content of Natural Waters in the Hydrologic Cycle. *Rev. of*
524 *Geophys.*, 2(1), 177-224, 1964.

525

526 Geprägs, P., M. E. Torres, S. Mau, S. Kasten, M. Römer, and G. Bohrmann:
527 Carbon cycling fed by methane seepage at the shallow Cumberland Bay,
528 South Georgia, sub-Antarctic, *Geochem. Geophys. Geosyst.*, 17, 1401–1418,
529 2016.

530

531 Holler, T., Wegener, G., Knittel, K., Boetius, A., Brunner, B., Kuypers, M. M.
532 M., & Widdel, F.: Substantial $^{13}\text{C}/^{12}\text{C}$ and D/H fractionation during anaerobic
533 oxidation of methane by marine consortia enriched in vitro. *Environ. Microbiol.*
534 *Rep.*, 1, 370-376, 2009.

535

536 James, R. H., Bousquet, P., Bussmann, I., Haeckel, M., Kipfer, R., Leifer, I.,
537 Niemann, H., Ostrovsky, I., Piskozub, J., Rehder, G., Treude, T., Vielstädte, L.
538 and Greinert, J.: Effects of climate change on methane emissions from
539 seafloor sediments in the Arctic Ocean: A review. *Limnol. Oceanogr*, special
540 issue, 2016.

541

542 Karl, D.M., Beversdorf, L., Bjorkman, K.M., Church, M.J., Martinez, A. &
543 Delong, E.F.: Aerobic production of methane in the sea, *Nature Geoscience*,
544 1, 473-478, 2008.

545

546 Karlsson, E. S., Charkin, A., Dudarev, O. Semiletov, I. P., Vonk, J. E.,
547 Sánchez-García, L., Andersson, A., and Gustafsson, Ö.: Carbon isotopes and
548 lipid biomarker investigation of sources, transport and degradation of
549 terrestrial organic matter in the Buor-Khaya Bay, SE Laptev Sea,
550 *Biogeosciences*, 8, 1865-1879, 2011.

551

552 Karlsson, E. et al.: Different sources and degradation state of dissolved,
553 particulate, and sedimentary organic matter along the Eurasian Arctic coastal
554 margin. *Global Biogeochemical Cycles*, 30(6), 898–919, 2016.

555

556 Kessler, J. D. et al. A persistent oxygen anomaly reveals the fate of spilled
557 methane in the deep Gulf of Mexico. *Science*, 331, 312–315, 2011.

558

559 Knittel, K.; Boetius, A. Anaerobic oxidation of methane: Progress with an
560 unknown process. *Annu. Rev. Microbiol.*, 63, 311–334, 2009.

561

562 Koch, K., C. Knoblauch, and D. Wagner: Methanogenic community
563 composition and anaerobic carbon turnover in submarine permafrost

564 sediments of the Siberian Laptev Sea, *Environ. Microbiol.*, 11(3), 657–668,
565 2009.

566

567 Kvenvolden, K. A.: Methane hydrates and global climate. *Glob. Biogeochem.*
568 *Cy.*, 2(3), 221–229, 1988.

569

570 Lammers, S., Suess, E.: An improved head-space analysis method for
571 methane in seawater, *Marine Chemistry* 47, 115-125, 1994.

572

573 Lessner, D. J.: Methanogenesis Biochemistry. In: *Encyclopedia of Life*
574 *Sciences (ELS)*. Chichester, UK: Wiley and Sons Ltd, 2009.

575

576 Mau, S., Brees, J., Helmke, E., Niemann, H. & Damm, E. Vertical distribution
577 of methane oxidation and methanotrophic response to elevated methane
578 concentrations in stratified waters of the Arctic fjord Storfjorden (Svalbard,
579 Norway). *Biogeosciences*, 10 6267–6278, 2013.

580

581 Nicolsky, D., Romanovsky, V. E., Romanovskii, N. N., Kholodov, A. L.,
582 Shakhova, N. E., & Semiletov, I. P.: Modeling sub-sea permafrost in the East
583 Siberian Arctic Shelf: The Laptev Sea region. *J. Geophys. Res.*, 117, F03028,
584 2012.

585

586 O'Connor, F. M., Boucher, O., edney, N., ones, C. D., Folberth, . A., Coppel,
587 R., Friedlingstein, P., Collins, W. J., Chappellaz, J., Ridley, J., & Johnson, C.
588 E.: Possible role of wetlands, permafrost and methane hydrates under future
589 climate change: a review. *Rev. Geophys.*, 48, RG4005, 2010.

590

591 Overduin, P. P., S. Liebner, C. Knoblauch, F. Günther, S. Wetterich, L.
592 Schirrmeister, H.-W. Hubberten, & M. N. Grigoriev: Methane oxidation
593 following submarine permafrost degradation: Measurements from a central
594 Laptev Sea shelf borehole, *J. Geophys. Res. Biogeosci.*, 120,965–978,
595 doi:10.1002/2014JG002862, 2015.

596

597 Prinzhofer, A., and E., Pernaton: Isotopically light methane in natural gas:
598 bacterial imprint or diffusive fractionation?, *Chemical Geology*, 142, 193-200,
1997.

599

600 Romanovskii, N. N., Hubberten, H.-W., Gavrilov, A. V., Eliseeva, A. A., &
601 Tipenko, G. S.: Offshore permafrost and gas hydrate stability zone on the
602 shelf of East Siberian Seas. *Geo-Mar. Lett.*, 25, 167-182, 2005.

603

604 Reeburgh, W. S. Oceanic methane biogeochemistry. *Chem. Rev.*, 107,
605 486–513, 2007.

606

607 Ruff, M., Szidat, S., Gäggeler, H. W., Suter, M., Synal, H.-A., & Wacker, L.:
608 Gaseous radiocarbon measurements of small samples, *Nucl. Instr. and Meth.*
609 *B*, 268, 790-794, 2010.

610 Ruppel, C.: Permafrost-associated gas hydrate: Is it really approximately 1%
611 of the global system?, *J. Chem. Eng. Data*, 60, 429–436, 2014.
612

613 Ruppel, C. D., and J. D. Kessler: The interaction of climate change and
614 methane hydrates, *Rev. Geophys.*, 55, doi:10.1002/2016RG000534, 2017.
615

616 Sapart, C. J., van der Veen, C., Vigano, I., Brass, M., van de Wal, R. S. W.,
617 Bock, M., Fischer, H., Sowers, T., et al and Röckmann, T. (2011).
618 Simultaneous stable isotope analysis of methane and nitrous oxide on ice
619 core samples. *Atm. Meas. Tech.*, 4, 2607- 2618.
620

621 Sasakawa, M., Tsunogai, U., Kameyama, S., Nakagawa, F., Nojiri, Y. and
622 Tsuda, A.: Carbon isotopic characterization for the origin of excess methane
623 in subsurface seawater, *Journal of Geophysical Research*, 113, C03012,
624 2008.
625

626 Semiletov I.P., Shakhova N. E., Sergienko V.I., Pipko I.I., and O. Dudarev:
627 On Carbon Transport and Fate in the East Siberian Arctic Land-Shelf-
628 Atmosphere System, *Environment Research Letters*, 7, 2012.
629

630 Semiletov et al., Acidification of East Siberian Arctic Shelf water through
631 addition of freshwater and terrestrial carbon. *Nature Geosciences*, 9, 361-365,
632 2016.
633

634 Schmitt, M., Faber, E., Botz, R., and Stoffers, P.: Extraction of methane from
635 seawater using ultrasonic vacuum degassing, *Anal. Chemistry* 63, vol. 5, 529-
636 532, 1991.
637

638 Schoell, M.: Multiple origins of methane on Earth. *Chemical Geology*, 71, 1-10,
639 1988.
640

641 Schuur, E.A.G., Abbott, B. W., Bowden, W. B., Brovkin, V., Camill, P.,
642 Canadell et al. and Zimov, S. A.: Expert assessment of vulnerability of
643 permafrost carbon to climate change. *Climatic Change*, 119(2), 359-374,
644 2013.
645

646 Shakhova, N., I. Semiletov, and G. Panteleev: The distribution of methane on
647 the Siberian Arctic shelves: Implications for the marine methane cycle,
648 *Geophysical Research Letters*, 32, L09601, 2005.
649

650 Shakhova N.E., Nicolsky D., and I. P. Semiletov: On the current state of sub-
651 sea permafrost in the East-Siberian Shelf testing of modeling results by
652 observational data. *Transactions of Russian Academy of Sciences, Vol. 429*
653 *(5)*, 2009 (translated in English by Springer), 2009.
654

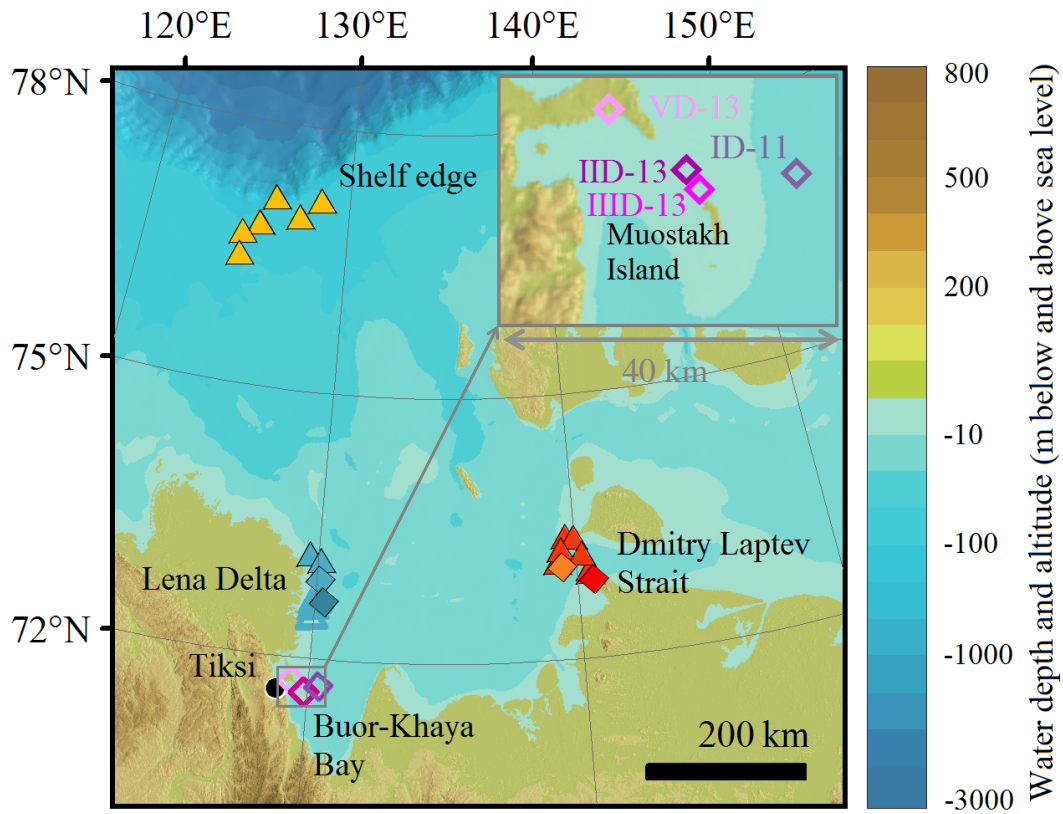
655 Shakhova, N., Semiletov, I., Leifer, I., Rekant, P., Salyuk, A., & Kosmach, D.
656 Geochemical and geophysical evidence of methane release from the inner
657 East Siberian Shelf. *J. Geophys. Res.*, 115, C08007, 2010a.

658
659 Shakhova, N, I. Semiletov, A. Salyuk, V. Yusupov, D. Kosmach & O.
660 Gustafsson: Extensive methane venting to the atmosphere from sediments of
661 the East Siberian Arctic Shelf, *Science*, 327, 1246-1250, 2010b.
662
663 Shakhova, N., Semiletov, I., Leifer, I., , Sergienko, V., Salyuk, A., Kosmach,
664 D., Chernikh D., Stubbs Ch., Nicolsky D., Tumskey V., and O.
665 Gustafsson Ebullition and storm-induced methane release from the East
666 Siberian Arctic Shelf, *Nature Geosciences*, vol.7, No.1, 64-70, 2013.
667
668 Shakhova N., Semiletov, I., Sergienko, V., Lobkovsky, L., Yusupov, V.,
669 Salyuk, A., Salomatin, A., Chernykh, D., Kosmach, D., Panteleev, G.,
670 Nicolsky, D., Samarkin, V., Joye, S., Charkin, A., Dudarev, O., Meluzov, A.,
671 Gustafsson, O.: The East Siberian Arctic Shelf: towards further assessment of
672 permafrost-related methane fluxes and role of sea ice. *Phil. Trans. R. Soc.*
673 *A*, vol. 373: 20140451, 2015.
674
675 Steinle, L, Graves, C., Treude, T., Ferré, B., Biastoch, A., Bussmann, I.,
676 Berndt, C., Krastel, S., James, R.H., Behrens, E., Böning, C.W., Greinert, J.,
677 Sapart, C.J., Scheinert, M., Sommer, S., Lehmann, M.F. and Niemann, H.:
678 Water column methanotrophy controller by a rapid oceanographic switch.
679 *Nature Geoscience*, 8, 378-382, 2015.
680
681 Szidat, S., Salazar, G. A., Vogel, E., Battaglia, M., Wacker, L., Synal, H.-A.
682 and Türlér, A.: ¹⁴C analysis and sample preparation at the new Bern
683 Laboratory for the Analysis of Radiocarbon with AMS (LARA), *Radiocarbon*,
684 56, 561-566, 2014.
685
686 Tesi, T., Semiletov, I., Hugelius, G., Dudarev, O., Kuhry, P., and Gustafsson,
687 Ö.: Composition and fate of terrigenous organic matter along the Arctic land–
688 ocean continuum in East Siberia: Insights from biomarkers and carbon
689 isotopes, *Geochimica et Cosmochimica Acta*, 133, 235–256, 2014.
690
691 Tesi, T., I. Semiletov, O. Dudarev, A. Andersson, and Ö. Gustafsson: Matrix
692 association effects on hydrodynamic sorting and degradation of terrestrial
693 organic matter during cross-shelf transport in the Laptev and East Siberian
694 shelf seas, *J. Geophys. Res. Biogeosci.*, 121, 2016.
695
696 Thornton, B. F., M. Wik, and P. M. Crill: Double-counting challenges the
697 accuracy of high-latitude methane inventories, *Geophys. Res. Lett.*,
698 43,12,569–12,577, 2016.
699
700 Vonk, J. E., Sánchez-García, L., van Dongen, B. E., Alling, V., Kosmach, D.,
701 Charkin, A., Semiletov, I. P., Dudarev, O. V., Shakhova, N., Roos, P., Eglinton,
702 T. I., Andersson, A., & Gustafsson, Ö.: Activation of old carbon by erosion of
703 coastal and subsea permafrost in Arctic Siberia. *Nature*, 489, 137–140, 2012.
704

705 Vonk J.E., Semiletov, I.P., Dudarev O.V., Eglinton T.I., Andersson A.,
706 Shakhova N., Charkin A., Heim B., Gustafsson: Preferential burial of
707 permafrost derived organic carbon in Siberian-Arctic shelf waters, *J. Geophys.*
708 *Res.*, Vol. 119, N 12, P. 8410-8421, 2014.
709
710 Walter, K. M., J. P. Chanton, F. S. Chapin III, E. A. G. Schuur, and S. A.
711 Zimov: Methane production and bubble emissions from arctic lakes: Isotopic
712 implications for source pathways and ages, *J. Geophys. Res.*, 113, 305-315,
713 2008.
714
715 Wiesenburg, D. A., & Guinasso Jr., N. L.: Equilibrium solubilities of methane,
716 carbon monoxide and hydrogen in salt and sea water. *J. Chem. Eng. Data*,
717 24(4), 356-360, 1979.
718
719 Winterfeld, M., Laepple, T., and Mollenhauer, G.: Characterization of
720 particulate organic matter in the Lena River delta and adjacent nearshore
721 zone, NE Siberia – Part I: Radiocarbon inventories, *Biogeosciences*, 12,
722 3769-3788, 2015.
723
724 Whiticar, M. J.: Carbon and hydrogen isotope systematics of bacterial
725 formation and oxidation of methane. *Chem. Geo.*, 161, 291-314, 1999.
726
727 Yoshinaga, M. Y., T. Holler, T. Goldhammer, G. Wegener, J. W. Pohlman, B.
728 Brunner, M. M. M. Kuypers, K. Hinrichs, and M. Elvert: Carbon isotope
729 equilibration during sulphate-limited anaerobic oxidation of methane, *Nat.*
730 *Geosci.*, 7(3), 190–194, 2014.
731
732
733
734
735
736
737
738
739
740
741
742
743
744
745
746
747
748
749
750
751
752

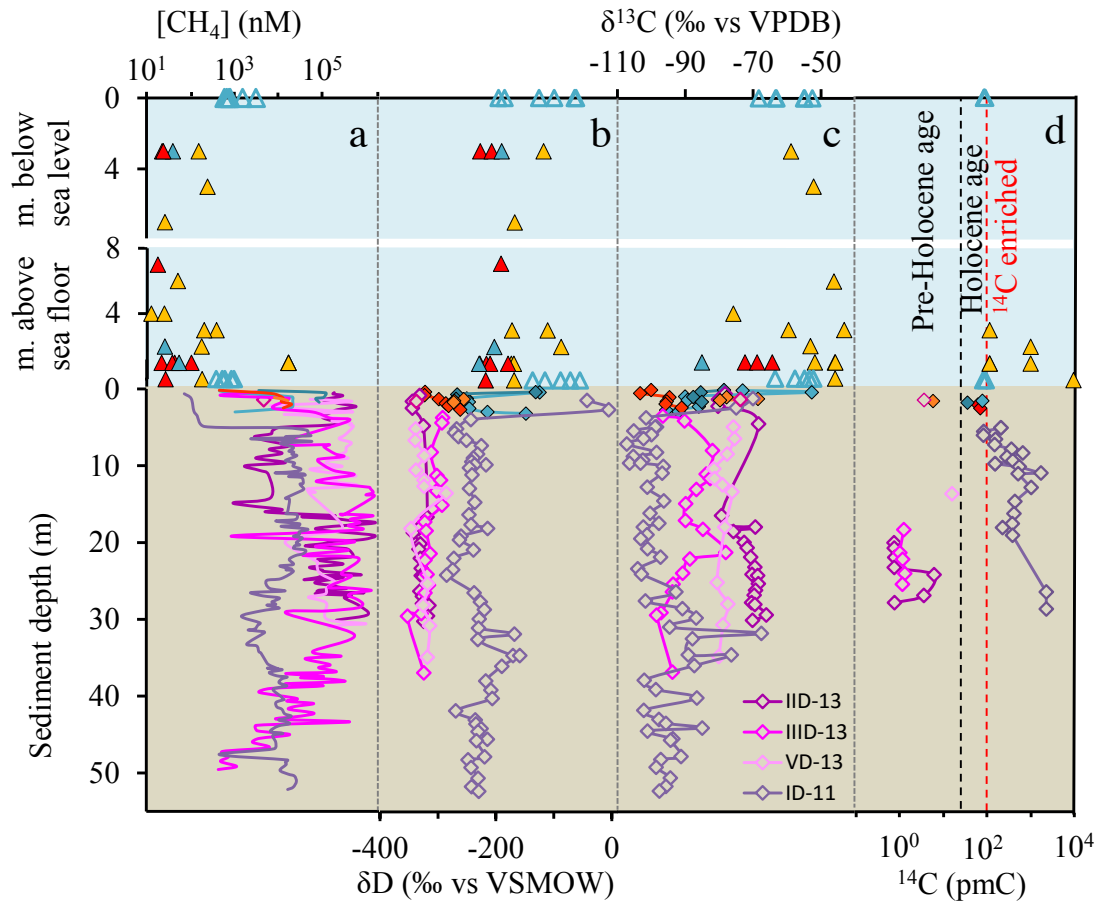
753
754
755
756
757
758

Figures



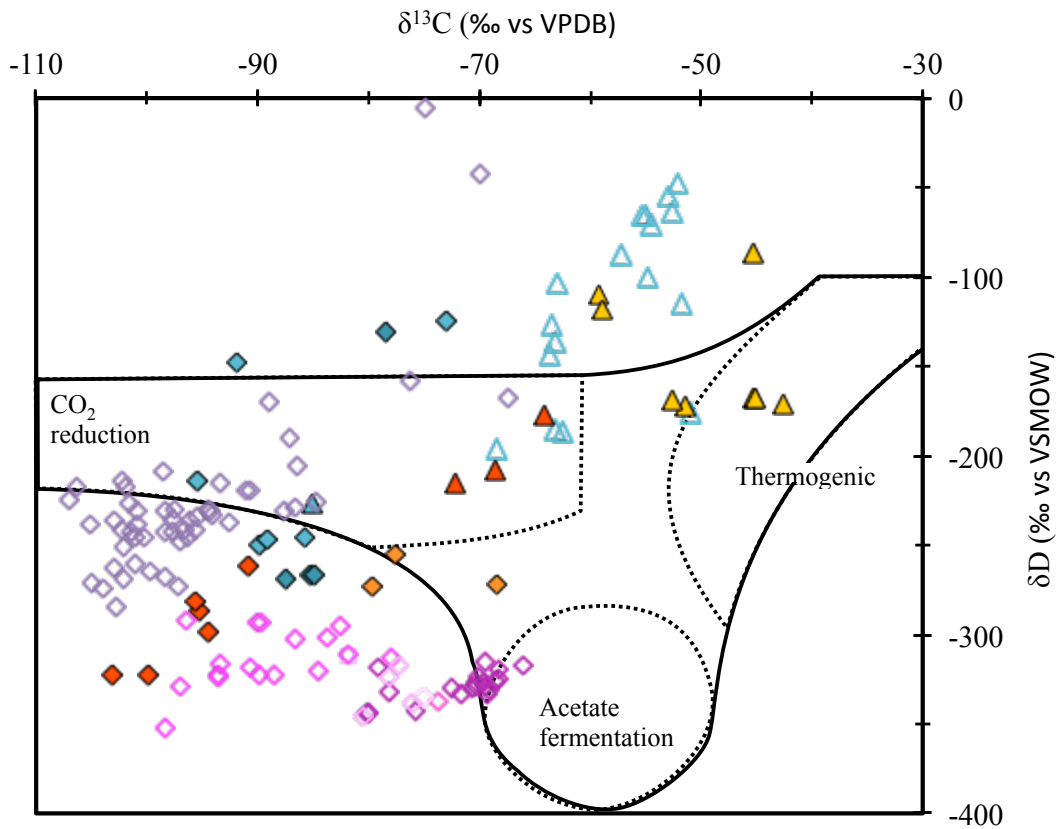
759
760
761
762
763

Figure 1: Sampling location. Water sampling (triangles), sediment drilling (diamonds). Summer sampling (close symbols) and winter sampling (open symbols). The color legends of the deep sediment cores are shown on the top right.



765
 766
 767
 768
 769
 770
 771
 772
 773
 774
 775

Figure 2: CH₄ data from sediment and overlying water sampled on the East Siberian Arctic Shelf. Water sampling (triangles), sediment cores (diamonds). Summer sampling (close symbols) and winter sampling (open symbols). Buor-Khaya Bay (purple, ID-11: non-ebullition site and IID-13, IID-13 and VD13 hotspot sites), Dmitry Laptev Strait (red and orange), Lena Delta (light blue) and Shelf Edge (yellow) (see Fig.1 for detailed location). (a) CH₄ concentrations, (b) δ¹³C (‰ vs VPDB), (c) δ¹³C (‰ vs VPDB), (d) ¹⁴C (pmC). The red dotted line corresponds to modern values (i.e., 100pmC) and the black dashed line corresponds to the onset of the Holocene (11,000 years BP). Note that y-axis for the water samples is divided in two sections. The upper part corresponds to the depth from the sea surface and the lower part corresponds to the depth from the seabed. See Fig. S1-S4 for the ice-bonded permafrost table depths and Table S1 for bathymetric information.



776

777

778

Figure 3: Dual-isotope CH₄ plot. Legend is similar to Fig.2. Areas delimited by black lines correspond to the three main CH₄ formation processes and their isotopic signatures (Whiticar, 1999).

779

780

781

782

783

784

785

786

787

788

789

790

791

792

793

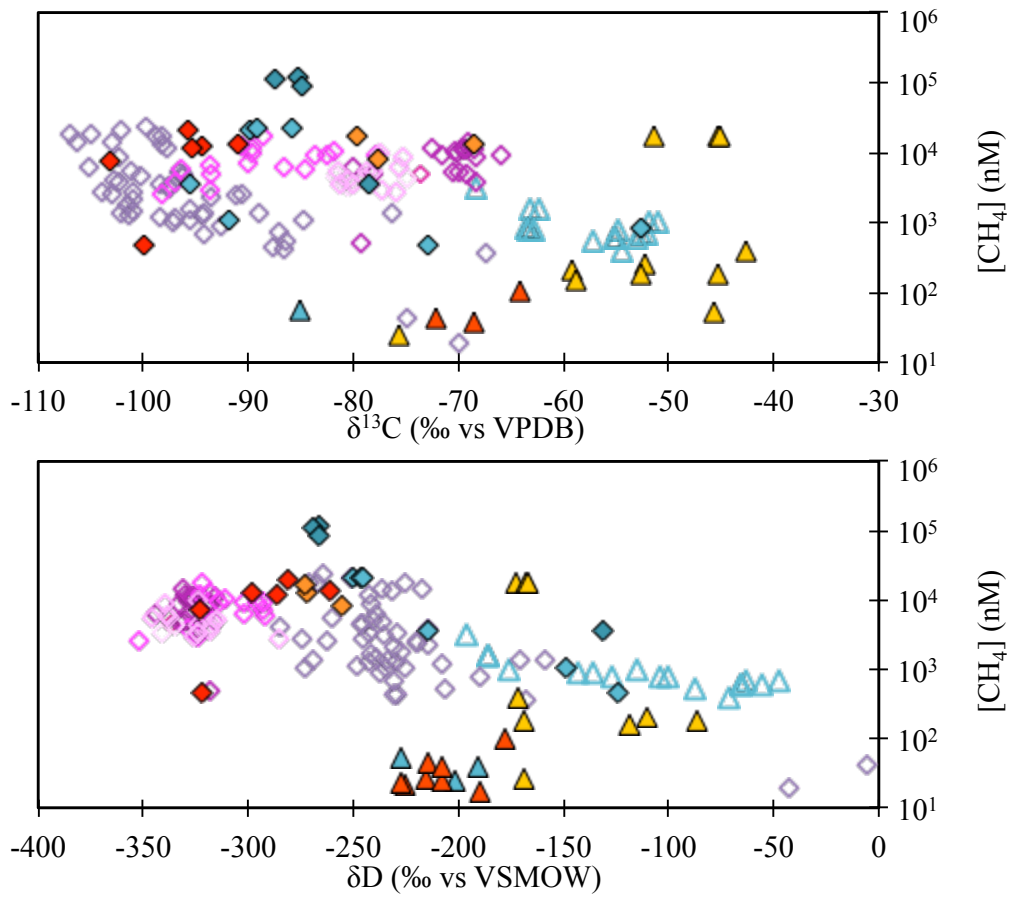
794

795

796

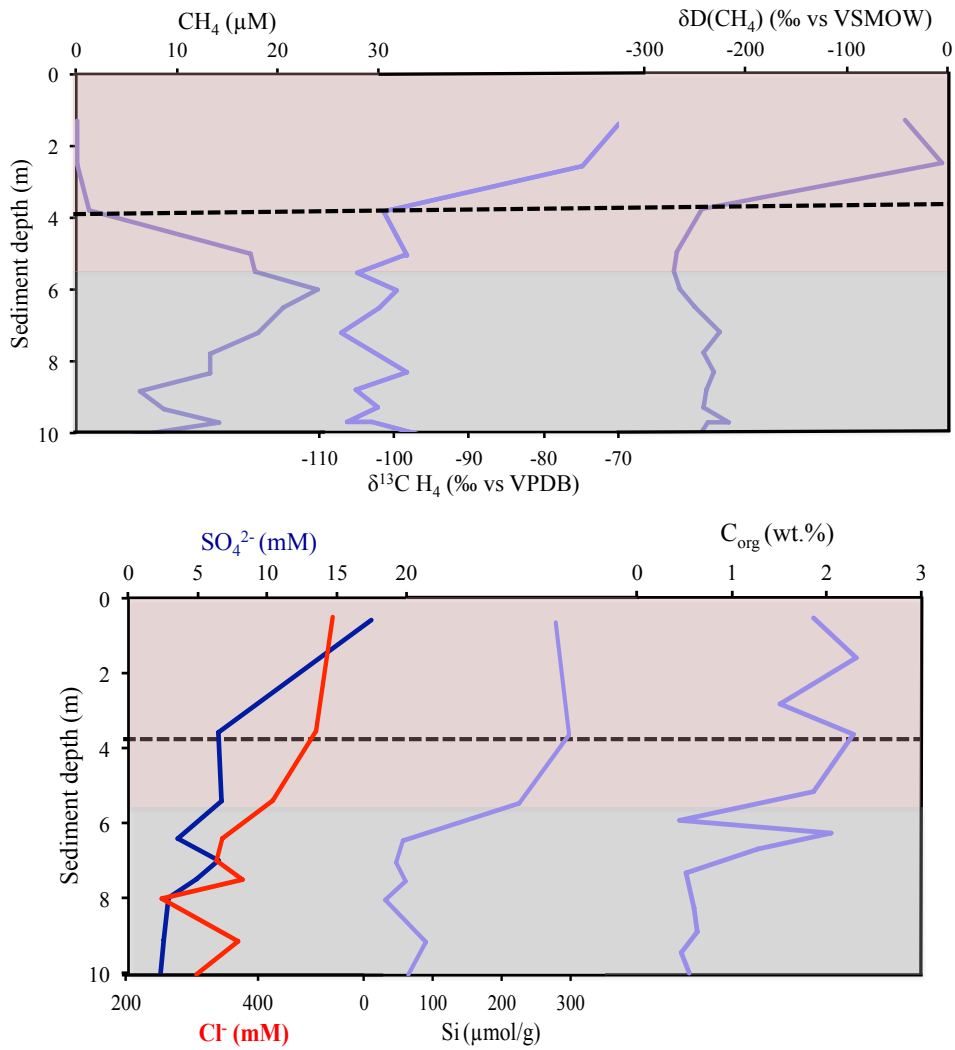
797

798



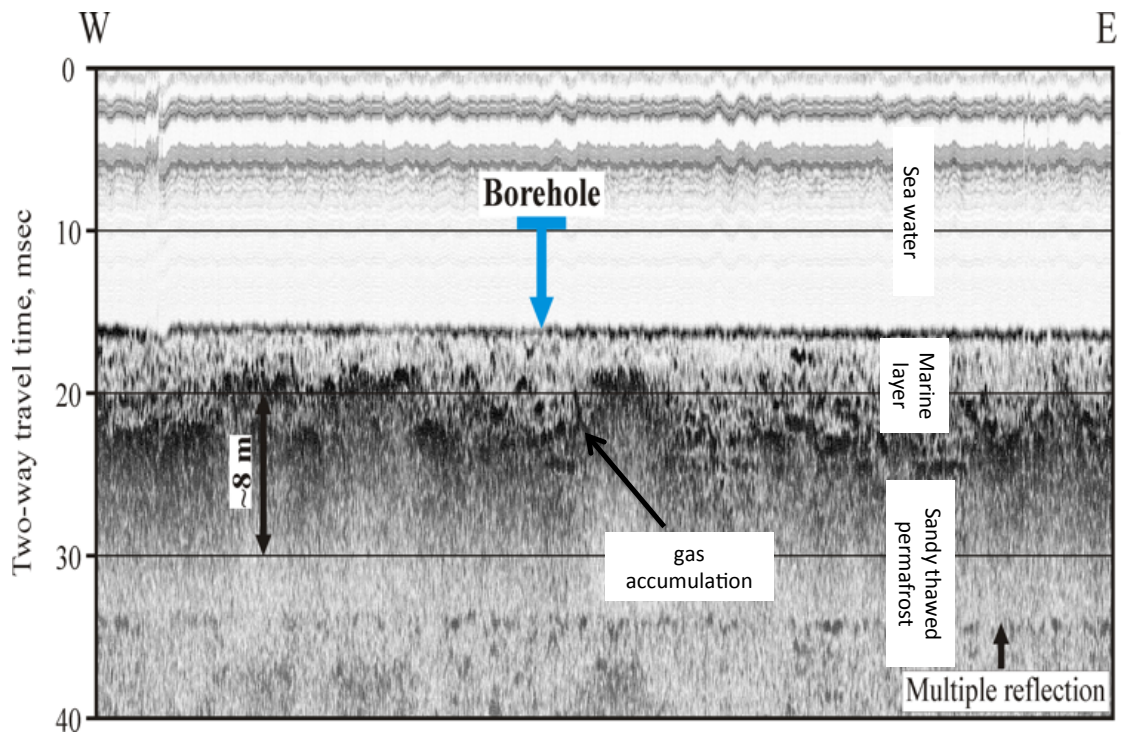
799
800
801
802
803
804

Figure 4: CH₄ concentration versus stable isotope plots. Water sampling (triangles), sediment cores (diamonds). Summer sampling (close symbols) and winter sampling (open symbols). Buor-Khaya Bay (purple, ID-11: non-ebullition site and IID-13, IID-13 and VD13 hotspot sites), Dmitry Laptev Strait (red and orange), Lena Delta (light blue) and Shelf Edge (yellow) (see Fig.1 for detailed locations and Table S1 for bathymetric information).



805
 806 **Figure 5: Close-up of the CH_4 concentration, stable isotope and other biogeochemical data of the**
 807 **surface of the non-ebullition sediment core ID-11, from the Buor-Khaya Bay. Red shaded area**
 808 **corresponds to the marine sediment deposited during the Holocene transgression and the grey**
 809 **shaded area corresponds to the thawed permafrost layer. The black dotted line corresponds to the**
 810 **depth where CH_4 oxidation starts to occur.**

811



812
813
814
815
816

Figure 6: Acoustic profile of the borehole of the ID-11 drilling site. Darker areas represent changes in density between the different horizontal layers (Sergienko et al., 2012). We assume that these changes in density indicate gas accumulation, because the sediment at this location is totally thawed, so it is very unlikely to be ice.

817